

Anion binding to a cationic europium(III) probe enables the first real-time assay of heparan sulfotransferase activity

Simon Wheeler,^a (0000-0003-0215-8648) Colum Breen,^a Sarah H. Hewitt,^a Erin Robertson,^a Yong Li,^b (0000-0002-5594-4434) David G. Fernig^b (0000-0003-4875-4293) and Stephen J. Butler^{*a} (0000-0001-8109-3330)

^aDepartment of Chemistry, Loughborough University, Epinal Way, Loughborough, LE11 3TU, UK

^bDepartment of Biochemistry, Institute for Integrative Biology, University of Liverpool, Liverpool, L69 7ZB, UK

*s.j.butler@lboro.ac.uk

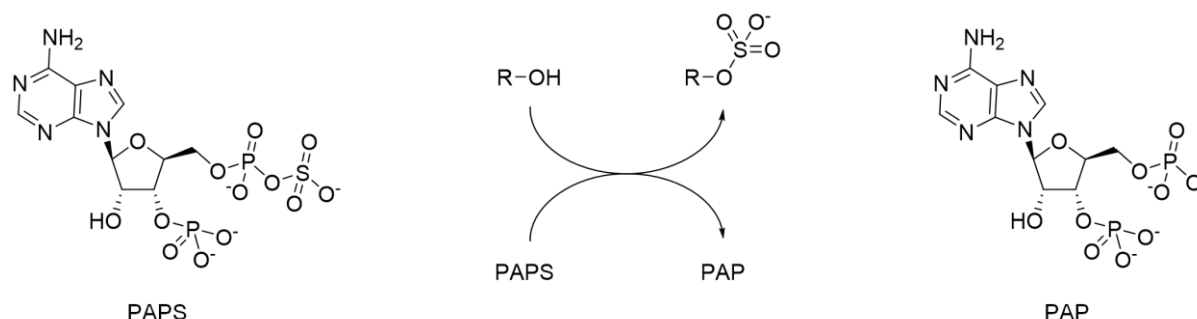
Abstract

Sulfotransferases constitute a ubiquitous class of enzyme which are poorly understood due to the lack of a convenient tool for screening their activity. These enzymes use the anion PAPS (adenosine-3'-phosphate-5'-phosphosulfate) as a donor for a broad range of acceptor substrates, including carbohydrates, producing sulfated compounds and PAP (adenosine-3',5'-diphosphate) as a side product. The few methods that have been published for monitoring these enzymes rely on specialised, expensive equipment. We present a europium(III)-based probe that binds reversibly to both PAPS and PAP, producing a larger luminescence enhancement with the latter anion. We exploit this greater emission enhancement with PAP to demonstrate the first direct real-time assay of a heparan sulfotransferase using multi-well plate format. The selective response of our probe towards structurally similar nucleoside phosphate anions, and over other anions, is investigated and discussed. This work opens the possibility of investigating more fully the roles played by this enzyme class in health and disease, including operationally simple inhibitor screening.

Introduction

The past two decades have seen a multitude of studies aimed at fundamental understanding of lanthanide complexes and at their exploitation as luminescent sensors and probes.^{1–6} When suitably ligated and irradiated with light in the UV or visible range, certain lanthanide(III) ions undergo an electronic excitation; relaxation of this excited state leads to luminescence.⁷ Such lanthanide complexes possess a range of qualities that make them particularly interesting and useful for sensing and imaging purposes, including their typically large pseudo-Stokes shifts, narrow emission linewidths and long emission lifetimes (millisecond range for europium and terbium).^{8,9} Anion responsive lanthanide complexes may be designed by introducing one or more vacant coordination sites at the metal centre; these are occupied by water molecules in aqueous solution which deactivate the Ln(III) excited state through vibration of their O-H bonds. Thus, coordination of a target anion at the metal centre displaces one or more water molecules, leading to an extension of the excited state lifetime and increase of the luminescence. Careful design of the ligating group(s) can give rise to remarkable

selectivity amongst anions, allowing sensors to be created that signal anion binding through modulation of emission intensity, lifetime and spectral form.^{1,6,10} In particular, it has proved possible to discriminate between very similar phosphate-containing biomolecules in complex aqueous solutions,¹¹ an area where we have been active.^{12–16}



Scheme 1 Sulfotransferase action Sulfotransferases add SO_3^- to hydroxyl or amino groups producing organic sulfates; PAPS functions as the donor yielding PAP as the by-product

Heparan sulfotransferases mediate the attachment of a sulfate group to an atom (usually oxygen, though sometimes nitrogen) in the heparanosan/heparan sulfate polysaccharide (Scheme 1). They exist in numerous isoforms with varying substrate preferences.¹⁷ The sulfated products of this reaction play important roles in cell communication¹⁸ and also feature in various pathologies including those of cancer,¹⁹ Alzheimer's²⁰ and the mucopolysaccharidoses.²¹ Heparan sulfotransferases belong to the wider group of sulfotransferases found across nature that use the universal sulfate donor compound PAPS (adenosine-3'-phosphate-5'-phosphosulfate),²² and produce PAP (adenosine-3',5'-diphosphate) as a by-product (Scheme 1). Very few methods have been disclosed for monitoring directly the activity of carbohydrate sulfotransferases. Those that have require radio-labelled substrates^{23–25} or specialized, expensive equipment.²⁶ All the published assays examine endpoints only and none are adaptable to high throughput format, probably accounting for the small numbers of reports of inhibitors of these enzymes.^{23,26,27} Further investigation of heparan sulfotransferases, including the vast potential of inhibitors as targets for drug discovery across a range of therapeutic areas, will likely remain slow unless an assay capable of both kinetic measurements and automated high throughput screening can be developed. We postulated that an assay based on emissive europium(III) probes could successfully fill this gap we had identified.

We recently reported a series of cationic europium(III) complexes bearing a sterically demanding 8-(benzyloxy)quinoline pendant arm that chelates the Eu(III) ion, offering a single coordination site suitable for the monodentate binding of phosphate and AMP (adenosine monophosphate).²⁸ We hypothesised that complexes of this design may be suitable for binding the structurally related phosphoanion, PAP, whilst showing a lower affinity for PAPS owing to the presence of the terminal cosulfate which would interact weakly with the hard Lewis acidic Eu(III) centre. Thus, we envisaged that PAP would induce a larger emission enhancement compared with PAPS or with any sulfated products, allowing us to monitor the PAPS/PAP ratio during the progress of the

sulfotransferase reaction. Our approach to monitoring sulfotransferase activity differs from previous work in that we target the small phosphoanion co-factor and the by-product derived from it, whereas other efforts have targeted the sulfated macromolecules. Similar supramolecular approaches utilising cucurbituril and calixarene host molecules have been developed for monitoring enzyme reactions, such as hydrolases and methyltransferases^{29–31} while we have previously used supramolecular anion recognition of phosphate-based species to monitor kinases.^{12,13} Here we report the initial results of our investigations into heparan sulfotransferases and disclose a europium(III)-based probe capable of monitoring one such enzyme in real-time, in principle independent of both substrate and product and so applicable to any sulfotransferase catalysed reaction

Results and Discussion

We began our work by examining the binding of PAP and PAPS to two monocationic lanthanide complexes (Figure 1) previously developed by us.²⁸ These have been shown to bind relatively strongly to inorganic phosphate and adenosine monophosphate (AMP) in aqueous solution, but do not bind sulfate, bicarbonate, lactate or acetate. Thus these complexes represented good starting points for the development of a luminescent probe for recognition of the structurally similar phosphoanion, PAP. We postulated that substituents on the distal benzene ring might affect the emission enhancements we observed in the presence of PAP and PAPS and thus complex EuBn, lacking the boronate ester group of EupBOH2, serves as an appropriate control complex to test our hypothesis.

Initially, we determined whether these two complexes could distinguish between PAP and PAPS by a differential luminescence response in 50 mM TRIS buffer at pH 7.4. Under these conditions, both anions induced an increase in overall emission intensity of both complexes, with the largest emission change occurring in the $\Delta J = 2$ (605 – 630 nm) emission band. Gratifyingly, PAP enhanced the emission of both complexes more than PAPS, as we expected. Compound EupBOH2 offered higher discrimination (Figure 1a) between PAP and PAPS, giving a 1.6-fold difference in emission intensity at 613 nm. In comparison, the binding of PAPS and PAP to complex EuBn gave a slightly reduced discrimination of 1.4-fold at 613 nm (Figure 1b).

Binding constants were determined for these complexes with PAP and PAPS in aqueous buffer at pH 7.4, by plotting the change in the intensity ratio of the $\Delta J = 2/\Delta J = 1$ bands against anion concentration and fitting the data to a 1:1 binding model. The binding titration data (Figure S1) indicated that there are only small differences in binding affinity of PAPS and PAP for either complex. Nevertheless, we considered our idea that substituents on the benzene ring affect anion discrimination to be vindicated and thus we set out to prepare a new complex functionalised with a *meta*-amino group on the benzene ring. Synthesis (Scheme 2) started with the alkylation of known³² phenol 1 with the requisite commercially available bromide followed by reduction of the resulting

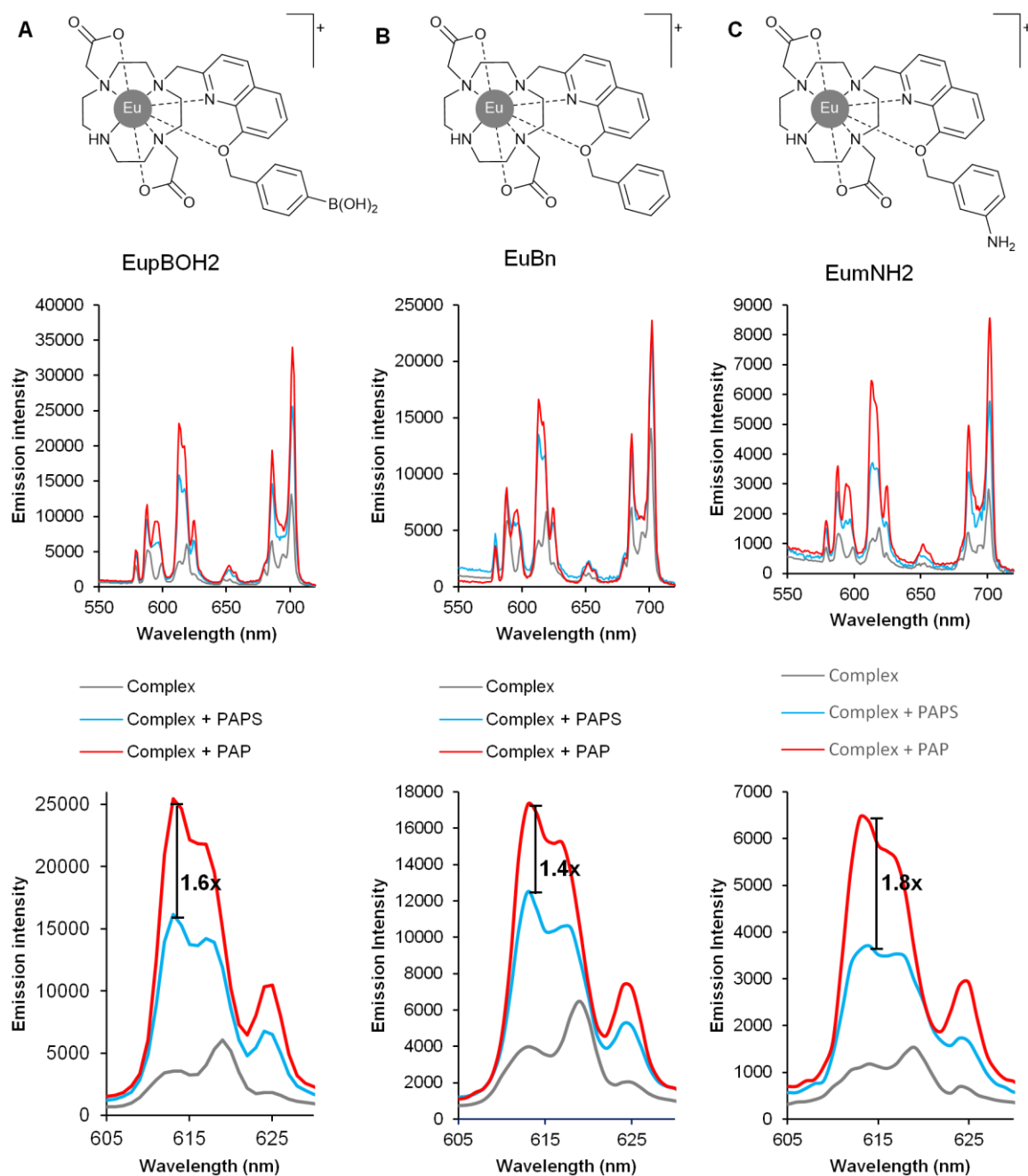
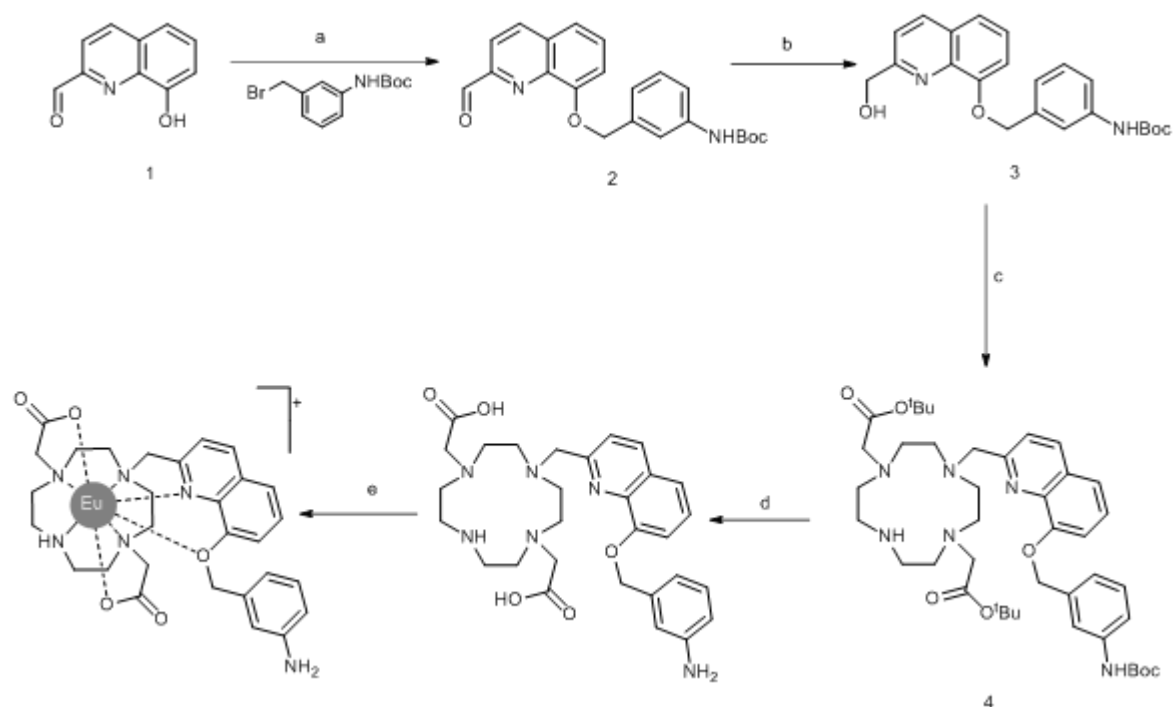


Figure 1. Structures of cationic Eu(III) complexes and their emission responses alone and in the presence of PAPS and PAP. All three Eu(III) probes give greater emission enhancements upon binding PAP compared with PAPS (**A-C**); removal of the boronate resulted in a loss of discrimination (**B** vs **A**) while installing an amino group increased it (**C** vs **A,B**). (All experiments conducted using 5 μ M probe, 250 μ M anion, in 50 mM TRIS at pH7.4, rt.)

Aldehyde **2** reduction to yield alcohol **3**. Activation of this gave the slightly unstable mesylate ester which was thus used immediately in an alkylation reaction with known³³ macrocycle to give protected ligand **4**. Simultaneous deprotection of the *tert*-butyl esters and Boc group with TFA yielded the ligand **5** which was heated with EuCl_3 to give our desired complex after purification by reverse-phase HPLC.



Scheme 2 Synthesis of **Eu-mNH2** Conditions: a) K_2CO_3 , DMF, rt, 2hr, 88%; b) NaBH_4 , MeOH, 0°C to rt, 55%; c) i) MsCl , Et_3N , DCM, 0°C to rt, ii) DO2A *tert*-butyl ester, K_2CO_3 , MeCN, 60°C , 18hr, 71% over two steps; d) 3:1 DCM/TFA, 18hr, quant; e) $\text{EuCl}_3 \cdot 6\text{H}_2\text{O}$, water, 60°C , $\text{pH} \geq 7.2$, prep HPLC, 9%.

Photophysical characterisation of this complex, **EumNH2** (Table 1, Figure S2) revealed a broad absorption band centred at 322 nm, identical to the unsubstituted compound with a very similar extinction coefficient. The emission spectrum was also similar to **EuBn**, characterised by two components in the $\Delta J = 1$ (585 – 600 nm) emission band and three components in the $\Delta J = 2$ (605 – 630 nm) band. We suspected that the much lower quantum yield of **EumNH2** and its smaller emission lifetime in water and D_2O (Table 1, Table S1) was caused by intramolecular photoinduced electron transfer (PET) from the nitrogen lone pair on the aniline ring quenching the europium excited state. Consistently, the emission from this complex was found to be highly pH-sensitive with much higher emission intensity observed at lower pH values (Figure S4). Further support for the involvement of the aniline nitrogen lone pair was the presence of a absorption band centred at 585 nm which is absent from the spectrum of the parent complex (compare Figure S2 and S3) and which disappears at low pH (Figure S4). We assign this band to an $n \rightarrow \pi^*$ transition. We attribute the emission enhancement and spectral form changes observed above pH 8 (Figure S4) to the coordination of hydroxide, but importantly the emission spectrum is stable in the pH range 6-8, rendering this compound potentially suitable for sulfotransferase assays.

The emission lifetime of parent and boronate complexes in water were similar and extended in D_2O as expected (Table 1, S1), giving rise to an estimation³⁴ of the number of bound water molecules, q , of 1 within experimental error. We interpret these non-integer values as suggesting dynamic behaviour of the bound waters, including interaction with outer sphere molecules. The emission lifetime of complex **EumNH2** was much shorter, consistent with PET quenching by the aniline nitrogen lone pair. Estimation

	EupBOH2	EuBn	EumNH2
λ_{max} (nm)	322	322	322
ϵ ($\text{M}^{-1} \text{cm}^{-1}$)	2900	2900	2500
Φ (%) ^a	1.2	1.5	0.3
$t_{\text{H}_2\text{O}}$ (ms) ^a	0.18	0.17	0.05
$t_{\text{D}_2\text{O}}$ (ms) ^a	0.25	0.23	0.07
q ^b	1.29	0.76	— ^c

Table 1 Photophysical parameters of the probes Experiments conducted in water, rt; quantum yield experiments conducted using probe solutions of 0.1 absorbance and calculated relative to a known standard; lifetime experiments conducted using 50 μM probe at rt λ_{ex} = 322nm, λ_{em} = 620nm. For full data see Table S1.

Notes: a errors in quantum yield and lifetime are $\pm 20\%$; b estimated using literature methods (see text); c very short emission lifetimes prevented accurate estimation of the hydration state

of the q value for such complexes becomes difficult as the emission lifetime begins to overlap with the water exchange timescale.³⁴ It is nonetheless significant that the emission lifetime was longer in D_2O suggesting that the complex is hydrated in the absence of anions.

We were pleased to discover that, despite being less emissive, the aniline complex outperformed both our initial boronate and unsubstituted benzene complex showing a 1.8-fold discrimination in emission between PAP and PAPS at 613nm (Figure 1c). Analysis of the anion binding titration data (Figure S1) indicated that EumNH2 has a genuine preference for binding PAP over PAPS ($\log K_a$ = 4.0 and 3.5, respectively), albeit with a modest 5-fold selectivity for the former anion.

We wished to confirm our hypothesis that the phosphate groups in PAPS and PAP coordinate to the Eu(III) ion and are thus responsible for the observed enhancement in emission and change in spectral form. First, we measured the emission response of EumNH2 in the presence of a small range of anions and found that inorganic phosphate was unique in giving a significant increase in luminescence especially in the $\Delta J=2$ band; other anions (sulfate, bicarbonate, nitrate, lactate and chloride) gave negligible changes in luminescence (Figure S5). Moreover, the emission spectral form changes observed in the presence of inorganic phosphate (Figure S5) matched that of PAP and PAPS, confirming that the phosphate-Eu(III) coordination is the primary interaction involved in the host-guest complexes involving PAP or PAPS.

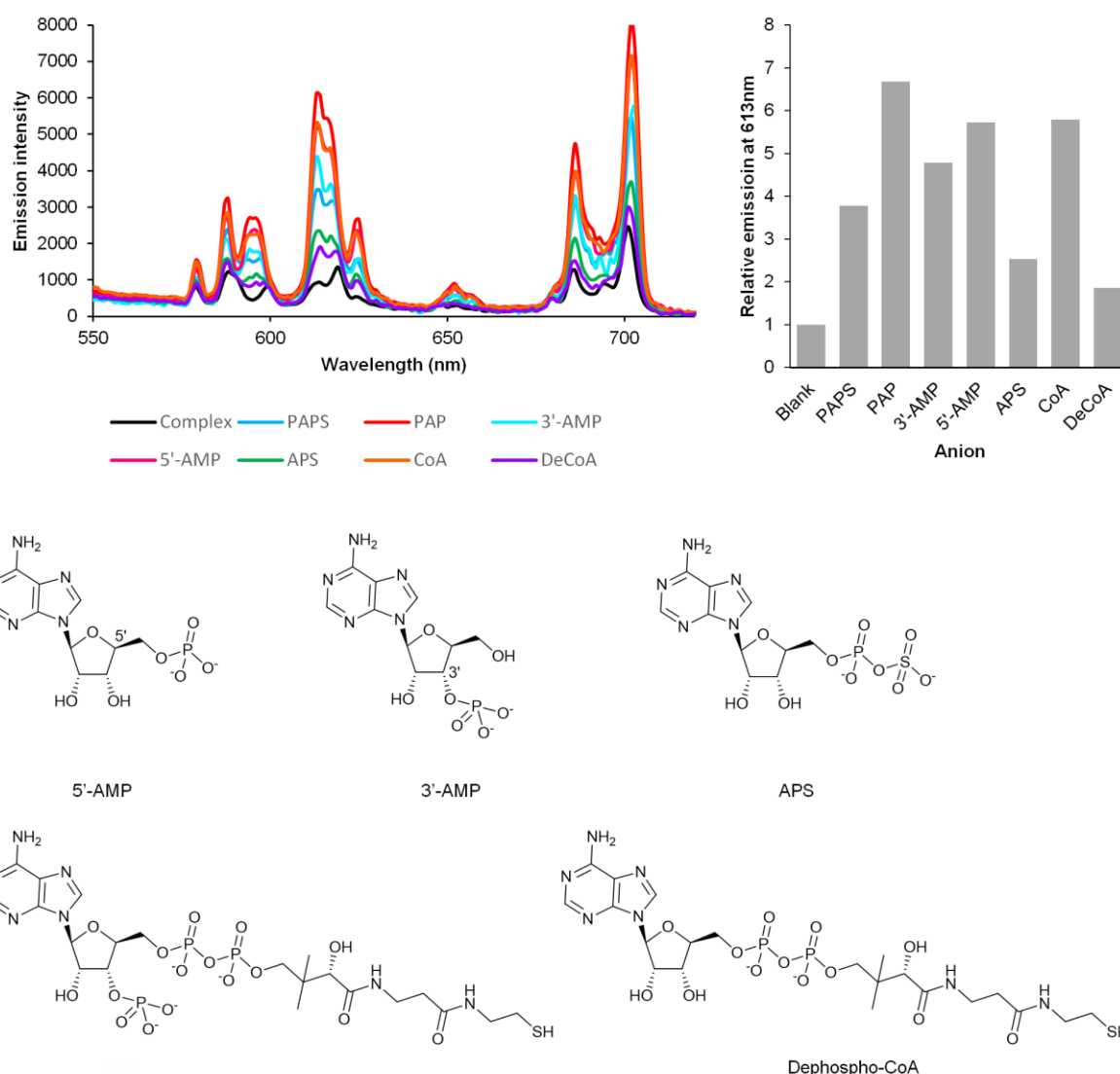


Figure 2 Investigation of anion binding modes by analysis of changes in the emission intensity and spectral form of **EmNH2**. Emission enhancement occurs if the anion possesses either a 3'-phosphate (PAPS, 3'-AMP, CoA), a 5'-phosphate (5'-CoA) or both (PAP); the absence of both 3'- and 5'-phosphates (APS, dephospho-CoA) results in very limited fluorescence enhancement. Experiments conducted using 5 μ M probe, 250 μ M anion in 50mM TRIS at pH7.4, rt. Very similar results were obtained for **EupBOH2** and **EuOBn** (see Figure S6).

We next examined a set of phosphorylated biomolecules structurally related to PAPS and PAP (Figure 2). The molecules tested that contained a simple phosphate group (5'-AMP, 3'-AMP, CoA) together with PAPS and PAP all gave significant luminescence enhancements (at least 4-fold) at 613nm. Structural analogues with a phosphate group bonded to an additional group but lacking an unconjugated phosphate (APS, dephospho-CoA) gave substantially lower enhancements in luminescence (ca. 2-fold). Similar trends in luminescence responses were obtained with the **EupBOH2** and **EuBn** (Figure S6). Molecules with only one unconjugated phosphate group (PAPS, 5'-AMP, 3'-AMP, CoA) gave a smaller luminescence enhancement than PAP, which has two phosphates. We thus tentatively conclude that PAP coordinates the Eu(III) complexes through both its phosphate groups. Conjugated phosphates (APS, dephospho-CoA) are also able to associate with the europium(III) ion, but the resulting host-guest structures are significantly less emissive.

With a PAP-selective complex in hand and a good understanding of its photophysical properties in aqueous solution, we proceeded to apply it to monitoring a sulfation reaction. We first evaluated the effect of our model acceptor substrate, heparin, on the luminescence of EumNH₂ and found that this heavily sulfated polysaccharide produced no change in the emission of the complex either alone or in the presence of PAPS or PAP (Figure S7). This is consistent with our finding discussed above that sulfate does not interact with our Eu(III) complex or affect its emission (Figure S5). The next step was to perform simulations of an enzyme reaction wherein our complexes were incubated with increasing molar ratios of PAP/PAPS, whilst keeping the total concentration of PAP and PAPS constant. In accord with the aim that our probes could ultimately be applied to high-throughput screening we conducted this work in 384-well plate format, taking advantage of the long emission lifetimes of the probes to record time-resolved measurements thereby increasing signal to noise ratio. All three Eu(III) complexes gave linear increases in time-resolved emission intensity of the $\Delta J=2$ band (Figure S8) as the mole fraction of PAP increases. Furthermore, the extent of the emission increase (determined by the gradient) was consistent with the emission differences we observed in our earlier fluorimetry experiments (Figure 1), confirming that our assay could transfer from quartz cuvette to polystyrene plate. These experiments also confirmed the aniline complex EumNH₂ as our most responsive, and therefore preferred, probe.

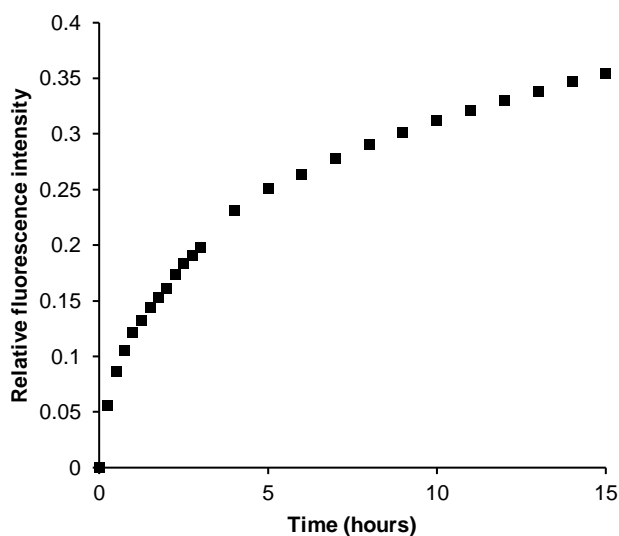


Figure 3 EumNH₂ can be used to monitor sulfation of heparin by HS3ST1 Data is from a representative example of two independent experiments conducted in triplicate and corrected for emission decay with identical mixture except omitting heparin. Experiments used 5 μ M probe, 250 μ M PAPS, 500 μ M heparin, 5 μ M HS3ST1, in 50mM TRIS at pH7.4, rt.

Next, we prepared a heparan sulfotransferase HS3ST1 (tagged with glutathione-S-transferase (GST) for ease of purification, Figure S9) and incubated the recombinant enzyme with PAPS and an excess of porcine intestinal mucosal heparin, one of its natural substrates, in the presence of our probe. While heparin molecules have already been sulfated by this enzyme *in vivo* prior to its isolation and use we reasoned that, as with all HSST reactions, sulfation of acceptor sites (in this instance on the C3 hydroxyl of glucosamine residues) is only partial.³⁵ Indeed, bovine intestinal

heparin has been shown to be a substrate *in vitro* for this enzyme.³⁶ We were delighted to observe a gradual increase in luminescence as PAPS was consumed and PAP was generated (Figure 3). This demonstrates the ability of our Eu(III) probe to function in a biological sulfation assay and thus renders the first example of real-time monitoring of a heparan sulfotransferase. Confirmation of the conversion of PAPS to PAP during the enzyme reaction was given by ¹H NMR spectroscopy, (Figure S10).

Conclusion

We have demonstrated proof-of-concept for the use of a new europium(III)-based anion receptor to monitor in real-time the activity of a heparan sulfotransferase. Previous assays^{23–26} have focussed on the macromolecular products of these reactions and required labour-intensive techniques and specialist equipment (and often a radiolabel) whereas our method examines the small anionic reaction partner and product, is independent of the acceptor, is label-free and relies solely on a standard plate reader. Our supramolecular approach to enzymatic monitoring exploits the ability of complex EumNH₂ to bind and discriminate between the structurally similar phosphoanions, PAP and PAPS, whilst showing no interference from sulfated biomolecules present in the bioassay.

Whilst this work brings the carbohydrate sulfotransferases, which are known to be druggable targets,²⁶ one step closer to high throughput inhibitor screening, our assay has some shortcomings. As noted above, the ability of the aniline nitrogen lone pair in EumNH₂ to act as a quencher of the europium(III) excited state means that our most selective probe is only weakly emissive and thus not very sensitive. Future work will focus on the design and synthesis of molecules that combine the selectivity of EumNH₂ with the sensitivity of the boronate probe. These studies are underway in our laboratories and will be reported in due course.

Experimental

General considerations

All chemicals were purchased from Cayman, Fluorochem, SiChem or Sigma-Aldrich and used without further purification.

NMR spectroscopy was carried out in the stated deuterated solvent using a JEOL ECS-400 (¹H at 399.78 MHz, ¹³C at 100.53 MHz) or a JEOL–ECS-500 spectrometer (¹H at 500.16 MHz, ¹³C at 125.77 MHz) spectrometer at 293 K. Chemical shifts are expressed in ppm and are adjusted to the chemical shift of the residual NMR solvent resonances (CDCl₃: ¹H δ = 7.26 ppm, ¹³C δ = 77.16 ppm or CD₃OD: ¹H δ = 3.31 ppm, ¹³C δ = 49.00 ppm).

All complexes were stored as 1 mM solutions in distilled water at -20 °C and diluted solutions prepared from these.

UV-Vis spectroscopy was performed using a Shimadzu UV-1800 instrument. Molar extinction coefficients were calculated using the Beer-Lambert law.

Luminescence spectroscopy was performed using a Camlin Photonics luminescence spectrometer with FluoroSENS version 3.4.7.2024 software. Emission spectra were obtained using a 40 μ L Hellma® Analytics quartz cuvette with excitation at 322nm and reading emission in the range 550-720nm using an integration time of 0.1s, increment of 1nm and excitation and emission slits of 0.5nm. Quantum yields were measured using quinine sulfate in 0.05 M H₂SO₄ as a standard (Φ_{em} = 0.59, λ_{ex} = 350 nm).³⁷ Plate-based assays were conducted in FisherBrand black, polystyrene 384-well plates with a maximum volume of 44 μ L per well.

Complex synthesis

Boronate and parent complexes were prepared as previously described²⁸ Complex EumNH₂ was prepared as follows:

Compound2

To a stirred solution of phenol **1** (200mg, 1.15mmol) in DMF (10mL) was added K₂CO₃ (235mg, 1.7mmol). After 5 minutes bromide (395mg, 1.38mmol) was added dropwise as a solution in DMF (2mL). After 1 hour the reaction was diluted with water (50mL) and extracted with EtOAc (3x15mL). Combined organics were washed with brine, dried over MgSO₄ and evaporated to a yellow oil that was purified by chromatography over SiO₂ (20g) eluting with 10-25% EtOAc/40-60 petroleum ether. Relevant fractions were combined, evaporated and dried under high vacuum to yield product **2** as an off-white solid (449mg, 1.01mmol, 88%). ¹H NMR (500MHz, CDCl₃): 1.49 (9H, s, H¹⁸), 5.44 (2H, s, H⁹), 6.55 (1H, bs, NH), 7.12 (1H, dd, J=7.8, 1.1Hz, H⁷), 7.20 (1H, m, H¹⁵), 7.27-7.32 (2H, m, H⁶, H¹³), 7.45 (1H, dd, J=8.3, 1.0Hz, H⁵), 7.52 (1H, m, H¹⁴), 7.60 (1H, s, H¹¹), 8.06 (1H, d, J=8.4Hz, H³), 8.26 (1H, d, J=8Hz, H⁴), 10.31 (1H, d, J=0.9Hz, H¹⁹). ¹³C NMR (126MHz, CDCl₃): 28.4 (C¹⁸), 71.0 (C⁹), 80.7 (C¹⁷), 111.1 (C⁷), 116.8 (C¹¹), 117.9 (C³), 118.0 (C¹³), 120.0 (C⁵), 121.5 (C¹⁵), 129.5 (C¹⁴), 129.7 (C⁶), 131.5 (C^{4a}), 137.3 (C⁴), 137.7 (C¹⁰), 138.9 (C¹²), 140.4 (C^{8a}), 151.7 (C⁸), 152.8 (C²), 155.2 (C¹⁶), 171.2 (C¹⁹). HRMS: C₂₂H₂₃N₂O₄⁺ requires 379.1652, found 379.1652

Compound3

To a stirred suspension of aldehyde **2** (430mg, 1.14mmol) in MeOH (20mL) under 1 atmosphere of N₂ and cooled in an ice-bath was added NaBH₄ (64mg, 1.5mmol) causing effervescence. After 1 hour the reaction was diluted with sat. aq. NH₄Cl (20mL) and extracted with EtOAc (3x15mL). Combined organics were washed with brine, dried over MgSO₄ and evaporated to a yellow oil that was purified by chromatography over SiO₂ eluting with EtOAc. Relevant fractions were combined, evaporated and dried under high vacuum to yield product **3** as an off-white solid (244mg, 0.64mmol, 56%). ¹H NMR (500MHz, CDCl₃): 1.49 (9H, s, H¹⁸), 4.55 (1H, bs, OH), 4.92 (2H, s, H¹⁹), 5.31 (2H, s, H⁹), 6.65 (1H, bs, NH), 7.08 (1H, dd, J=5.4, 3.6Hz, H⁷), 7.18 (1H, d, J=8.4Hz, H¹⁵), 7.28 (1H, m, H¹⁴), 7.30-7.34 (2H, m, H³, H¹³), 7.36-7.39 (2H, m, H⁵, H⁶), 7.56 (1H, bs, H¹¹), 8.08 (1H, d, J=8.4Hz, H⁴). ¹³C NMR (126MHz, CDCl₃): 28.4 (C¹⁸), 64.6 (C¹⁹), 70.8 (C⁹), 80.6 (C¹⁷), 111.1 (C⁷), 117.0 (C¹¹), 117.9 (C¹³), 119.0 (C³), 120.1 (C⁵), 121.5 (C¹⁵), 126.5 (C¹⁴), 128.9 (C^{4a}), 129.3 (C⁶), 136.8 (C⁴), 138.1 (C¹⁰), 138.8 (C¹²), 139.1 (C^{8a}), 152.8 (C⁸), 154.1 (C²), 158.2 (C¹⁶). HRMS: C₂₂H₂₅N₂O₄⁺ requires 381.1089, found 381.1807

Compound4

To a stirred solution of alcohol **3** (294mg, 0.77mmol) in DCM (10mL) cooled in an ice-bath was added Et₃N (162μL, 1.16mmol) followed by MsCl (72μL, 0.93mmol). After 1 hour fresh portions of Et₃N (81μL, 0.58mmol) and MsCl (36μL, 0.46mmol) were added. After a further 1 hour the reaction was washed with water (2x15mL), then with brine (20mL), dried over MgSO₄ and evaporated to give a yellow gum which was used without further purification. ¹H NMR (500MHz, CDCl₃): 1.49 (9H, s, H¹⁸), 3.14 (3H, s, H²⁰), 5.33 (2H, s, H¹⁹), 5.57 (2H, s, H⁹), 6.61 (1H, bs, NH), 7.08 (1H, dd, J=7.0, 1.9Hz, H⁷), 7.15 (1H, d, J=7.3Hz, H¹⁵), 7.26-7.35 (2H, m, H¹³, H¹⁴), 7.38-7.45 (2H, m, H⁵, H⁶), 7.55 (1H, d, J=8.5Hz, H³), 7.56 (1H, bs, H¹¹), 8.18 (1H, d, J=8.5Hz, H⁴).

To a stirred solution of mesylate (445mg, 0.95mmol) in MeCN (40mL) was added K₂CO₃ (394mg, 2.85mmol) followed by DO2A-*tert* butyl ester (380mg, 0.95mmol) and the mixture stirred at 60°C for 18 hours. The reaction mixture was cooled and centrifuged. The liquours were decanted and the solid washed with DCM (2x10mL). Combined liquids were evaporated to give a yellow gum which was purified by column chromatography over SiO₂ (40g) eluting with EtOAc then with 95:5:0.5 to 90:10:1 to 80:20:5 DCM/MeOH/880 NH₃. Relevant fractions were combined and evaporated to yield product **4** as an off-white foam (513mg, 0.67mmol, 71%). ¹H NMR (500MHz, CD₃OD): Compound **4** present as two rotamers in approximate ratio 4:1 1.37 and 1.48 (together 9H, s, H¹⁸, H²⁷), 2.38-3.10 (20H, m, H²⁰⁻²⁴), 3.60 and 3.93 (together 2H, s, H¹⁹), 5.18 and 5.31 (together 2H, s, H⁹), 6.70-7.89 (9H, m, NH, H³, H⁴⁻⁷, H¹¹, H¹³⁻¹⁵), 8.06 and 8.31 (together 1H, d, J=8.5Hz, H⁴). ¹³C NMR (126MHz, CD₃OD): some peaks doubled due to presence of rotamers 31.0 and 31.3 (C¹⁸ and C²⁷), 47.8, 52.8, 53.4 and 57.4 (C²⁰⁻²³), 59.0 and 59.1 (C²⁴), 63.8 and 64.6 (C¹⁹), 75.2 and 75.6 (C⁹), 83.7 and 85.1 (C²⁶), 85.0 and 85.3 (C¹⁷), 114.3 and 115.2 (C⁷), 123.2 (C¹¹), 123.5 (C¹³), 124.3 and 124.5 (C³), 127.5 and 127.6 (C¹⁵), 130.3 and 130.7 (C¹⁴), 132.3 and 132.6 (C^{4a}), 132.8 and 133.4 (C⁶), 140.6 and 141.1 (C⁴), 141.4 (C¹⁰), 143.3 and 143.5 (C¹²), 144.3 (C⁸), 157.7 (two peaks, C²), 157.9 (C^{8a}), 161.4 and 161.5 (C¹⁶), 174.7 and 174.9 (C²⁵). HRMS: C₄₂H₆₂N₆O₇⁺ requires 763.4674, found 763.4753

Compound 5

To a stirred solution of protected ligand **4** (500mg, 0.66mmol) in DCM (7.5mL) was added TFA (2.5mL) and stirring continued for 18 hours. After this time the solvent was removed *in vacuo* and the residue co-evaporated from DCM (5x10mL) to yield a brown gum corresponding to ligand **5** as the 3TFA salt (589mg, 0.66mmol, quant.), which was used in the next step without further purification. ¹H NMR (400MHz, CD₃OD): 2.71-4.25 (20H, m, H²⁰⁻²⁴), 4.77 (2H, s, H¹⁹), 5.37 (2H, s, H⁹), 7.20 (1H, H¹⁵), 7.26 (1H, dd, J=5.7, 3.3Hz, H¹³), 7.34-7.59 (H⁵⁻⁷, H¹¹, H¹⁴), 7.62 (1H, d, J=8.5Hz, H³), 8.34 (1H, d, J=8.5Hz, H⁴). ¹³C NMR (126MHz, CD₃OD) 42.5 (C²⁴), 48.8, 49.3, 52.1, 52.9 (C²⁰⁻²³), 57.4 (C¹⁹), 69.9 (C⁹), 110.4 (C⁷), 116.8 (q, J=291Hz, TFA CF₃), 119.4 (C¹³), 119.7 (C³), 119.8 (C¹¹), 122.3 (C⁵), 124.3 (C¹⁵), 127.6 (C¹⁴), 127.8 (C⁶), 129.2 (C¹⁰), 129.9 (C^{4a}), 137.8 (C⁴), 139.35 (C¹²), 139.42 (C^{8a}), 150.2 (C⁸), 154.1 (C²), 161.5 (q, J=35Hz, TFA C=O), 173.7 (C²⁵). HRMS: C₂₉H₃₈N₆O₅⁺ requires 551.2976, found 551.297.

EumNH2

Ligand **5**·3TFA (53mg, 0.059mmol) was dissolved in water (2mL) and the pH adjusted to 8.7 with 2M NaOH(aq). EuCl₃·6H₂O (23mg, 0.063mmol) was added causing a sharp drop in pH which was readjusted to 8.7 using 2M NaOH(aq). The reaction mixture was heated at 60°C for 18 hours maintaining pH ≥ 7.2. The reaction was centrifuged and the supernatant purified by preparative reverse-phase HPLC (Waters 1525 Binary HPLC pump controlled by the Waters Breeze 2 HPLC

system software, XBridge C18 (5 μ m OBD 19 \times 100 mm) column at a flow rate of 17 mL/min, gradient: 0-100% MeCN in 50mM $\text{NH}_4\text{HCO}_3(\text{aq})$ over 15mins, detection using a Waters 2489 UV/Visible detector operating at 254 nm, $t_R = 6.07$ mins). Solvent was removed by evaporation and then lyophilisation to yield complex **5** as a white solid (3.7mg, 0.005mmol, 9%). HRMS: $\text{C}_{29}\text{H}_{36}\text{EuN}_6\text{O}_5^+$ requires 701.1948, found 701.1951 $\lambda_{\text{max}} = 322\text{nm}$, $\epsilon = 2500 \text{ M}^{-1} \text{ cm}^{-1}$, $\phi = 0.3\%$, $\tau_{\text{H}_2\text{O}} = 0.05 \text{ ms}$, $\tau_{\text{D}_2\text{O}} = 0.07 \text{ ms}$

Preparation of GST-HS3ST1

The cDNA fragment encoding the sulfotransferase HS3ST1 (O35310_48-311) used previously by others³⁸ was purchased from Thermo Fisher Scientific (Thermo Fisher, UK). EcoRI and NotI were used as restriction sites for inserting the HS3ST1 encoding fragment into the pGEX4T3 vector. HS3ST1 was expressed in C41 (DE3) strain of *Escherichia coli* and induced with 200 μ M isopropyl 1-thio- β -D-galactopyranoside (IPTG) at 22°C overnight.³⁸ The cells were collected by centrifugation for 15 min at 4,150x g and resuspended in lysis buffer (100 mM NaCl, 50 mM Tris-Cl, pH 7.4) prior to cell breakage by sonication (six cycles of 30 s sonication and 30 s rest, on ice). Purification was achieved by applying the lysate sequentially to with two columns. First, a 2 mL glutathione resin (Genscript Biotech Corporation, Netherlands) self-packed column, washed with 100 mM NaCl, 50 mM Tris, pH 7.4 was eluted with 10 mM reduced glutathione, 100 mM NaCl, 50 mM Tris, pH 7.4. Second, the eluted fraction was applied to a 1 mL heparin (Affi-Gel hep, Bio-Rad, UK) self-packed column, washed with 50 mM NaCl, 50 mM Tris, pH 7.4 and, and eluted with 600 mM NaCl, 50 mM Tris, pH 7.4. Protein was quantified from its absorbances at 280 nm, using the extinction coefficient calculated for the amino acid sequence, snap frozen in liquid nitrogen and stored in aliquots at -80°C.

Luminescence experiments

Luminescence spectra were recorded on a Camlin Photonics luminescence spectrometer with FluoroSENS version 3.4.7.2024 software. Emission spectra were obtained using a 40 μ L Hellma Analytics quartz cuvette. Excitation light was set at 322 nm and emission recorded in the range 550 – 720 nm using an integration time of 0.5 seconds, increment of 1.0 nm, excitation slit of 0.2 nm and emission slit of 0.5 nm.

Emission lifetime measurements were performed on the FluoroSENS instrument. Measurements were taken of 40 μ L of 5 μ M samples of Eu(III) complexes in 50 mM TRIS at pH 7.4. Measurements were obtained by indirect excitation of the Eu(III) ion *via* the quinoline antennae using a short pulse of light at 322 nm followed by monitoring the integrated intensity of the light emitted at 620 nm, with 500 data points collected over a 5 millisecond time period. The decay curves were plotted in Origin Labs 2019 version 9.6.0.172, and fitted to the equation:

$$I = A_0 + A_1 e^{-kt} \quad (1)$$

where I is the intensity at time, t , following excitation, A_0 is the intensity when decay has ceased, A_1 is the pre-exponential factor and k is the rate constant for the depopulation of the excited state.

The hydration state, q , of the Eu(III) complexes was determined using the modified Horrocks equation³⁴:

$$q(\text{Eu}) = 1.2 (1/\tau_{\text{H}_2\text{O}} - 1/\tau_{\text{D}_2\text{O}} - 0.25 - 0.075n) \quad (2)$$

where $\tau_{\text{H}_2\text{O}}$ and $\tau_{\text{D}_2\text{O}}$ are the emission lifetime times in water and D_2O , respectively, and n is the number of carbonyl-bound amide NH groups.

Anion Screening Studies

Stock solutions of Eu(III) complexes were diluted to 5 μM using 50 mM TRIS buffer. 40 μL was placed in a quartz cuvette and the emission spectrum recorded. 1 μL of 10 mM anion solution in distilled water was added (final anion concentration 250 μM) and the emission recorded again. For inorganic anions (Figure S5) 1.6 μL of a 25 mM solution in HEPES was used, final concentration 1 mM.

Anion binding titrations

Anion binding titrations were carried out in 50 mM TRIS buffer at pH 7.4. Stock solutions of PAPS and PAP containing Eu(III) complex (5 μM) were made up at 0.1, 1 and 5 mM anion. The appropriate anion stock solution was added incrementally to 40 μL of Eu(III) complex (5 μM) and the emission spectrum was recorded after each addition. The ratio of emission bands 605 – 630 nm/ 585 – 600 nm ($\Delta J = 2 / \Delta J = 1$) was plotted as a function of anion concentration. The data was analysed using a nonlinear least-squares curve fitting procedure, based on a 1:1 binding model described by the equation:

$$FB = \frac{\frac{1}{K_a} + [A] + [Eu] - \sqrt{(\frac{1}{K_a} + [A] + [Eu])^2 - 4[A][Eu]}}{2[Eu]}$$

where FB is the fraction bound, calculated by $(I - I_0)/(I_1 - I_0)$ where I is the emission intensity at $[A]$, I_0 is the initial emission intensity, and I_1 is the final emission intensity. $[A]$ is the total concentration of anion in solution, $[Eu]$ is the total concentration of Eu(III) complex, K_a is the apparent binding constant.

Microplate-based enzyme simulations

Varying ratios of a solution of PAPS and PAP containing a 5 μM Eu(III) complex in 50 mM TRIS at pH 7.4 were added to a 384-well plate, in triplicate, to a total well volume of 40 μL . The plate was incubated for 10 minutes prior to reading. Time-resolved emission intensities were recorded in the range 610 – 630 nm (integration time of 60 – 400 μs) with excitation at 292 – 366 nm. The mean of the triplicate intensity values was plotted against the percentage of PAP. Error bars indicate the standard error in the mean value.

Microplate-based enzyme reactions

1.5 μL of 200 μM Eu-complex **5** was added to 58.5 μL of 20 μM GST-HS3ST1 and the mixture incubated at rt for 5 minutes. 6 \times 30 μL of a 5 μM solution of Eu-complex **5** in 50 mM TRIS were placed in a 384-well plate and to these were added the mixture of Eu-complex **5** and GST-HS3ST1 (final concentrations 5 μM and 5 μM respectively). 3 μL of either 50 mM TRIS or 100 mg/mL heparin were added to 3 wells

each and the plate allowed to incubate at rt for 5 minutes. 1 μ L of PAPS (10mM in distilled water) was added to each well (final concentration 250 μ M). The wells were scanned every 15 minutes for 3 hours then every hour for an additional 20 hours exciting at 292-364nm and measuring emission at 620 \pm 5nm. Emission change was calculated by normalising to the emission at t=0, averaging over replicates and subtracting the signal from wells with TRIS from the signal from wells with heparin.

Conflicts of interest

There are no conflicts of interest to declare.

Acknowledgements

This work was funded by a Biotechnology and Biotechnological Sciences Research Council Tools and Resources Development Grant [BB/T012099/1] to SB and DGF, a European Commission FET-OPEN grant [ArrestAD no.737390] to DGF and a Biotechnology and Biotechnological Sciences Research Council Industrial Biotechnology [BB/V003372/1] to DGF, SB and others. The authors wish to thank Rob Field for instigating this work.

References

- 1 S. J. Butler and D. Parker, *Chem. Soc. Rev.*, 2013, **42**, 1652–1666.
- 2 M. C. Heffern, L. M. Matosziuk and T. J. Meade, *Chem. Rev.*, 2014, **114**, 4496–4539.
- 3 J. C. G. Bünzli, *Coord. Chem. Rev.*, 2015, **293–294**, 19–47.
- 4 E. Mathieu, A. Sipos, E. Demeyere, D. Phipps, D. Sakaveli and K. E. Borbas, *Chem. Commun.*, 2018, **54**, 10021–10035.
- 5 D. Parker, J. D. Fradgley and K. L. Wong, *Chem. Soc. Rev.*, 2021, **50**, 8193–8213.
- 6 S. E. Bodman and S. J. Butler, *Chem. Sci.*, 2021, **12**, 2716–2734.
- 7 J. C. G. Bünzli and C. Piguet, *Chem. Soc. Rev.*, 2005, **34**, 1048–1077.
- 8 S. Faulkner, S. J. A. Pope and B. P. Burton-Pye, *Appl. Spectrosc. Rev.*, 2005, **40**, 1–31.
- 9 E. G. Moore, A. P. S. Samuel and K. N. Raymond, *Acc. Chem. Res.*, 2009, **42**, 542–552.
- 10 D. Parker, *Coord. Chem. Rev.*, 2000, **205**, 109–130.
- 11 C. M. G. Dos Santos, P. B. Fernández, S. E. Plush, J. P. Leonard and T. Gunnlaugsson, *Chem. Commun.*, 2007, **3389**, 3389–3391.
- 12 S. H. Hewitt, J. Parris, R. Mailhot and S. J. Butler, *Chem. Commun.*, 2017, **53**, 12626–12629.
- 13 S. H. Hewitt, R. Ali, R. Mailhot, C. R. Anttonen, C. A. Dodson and S. J. Butler, *Chem. Sci.*, 2019, **10**, 5373–5381.
- 14 S. H. Hewitt, R. Liu and S. J. Butler, *Supramol. Chem.*, 2018, **30**, 765–771.
- 15 S. H. Hewitt, G. Macey, R. Mailhot, M. R. J. Elsegood, F. Duarte, A. M. Kenwright and S. J. Butler, *Chem. Sci.*, 2020, **11**, 3619–3628.
- 16 R. Mailhot, T. Traviss-Pollard, R. Pal and S. J. Butler, *Chem. - A Eur. J.*, 2018, **24**, 10745–10755.
- 17 R. Wander, A. M. Kaminski, Y. Xu, V. Pagadala, J. M. Krahn, T. Q. Pham, J. Liu and L. C. Pedersen, *RSC Chem. Biol.*, 2021, **2**, 1239–1248.

- 18 M. C. Z. Meneghetti, A. J. Hughes, T. R. Rudd, H. B. Nader, A. K. Powell, E. A. Yates and M. A. Lima, *J. R. Soc. Interface*, 2015, **12**.
- 19 A. W. Y. Leung, I. Backstrom and M. B. Bally, *Oncotarget*, 2016, **7**, 55811–55827.
- 20 J. E. Sepulveda-Diaz, S. M. Alavi Naini, M. B. Huynh, M. O. Ouidja, C. Yanicostas, S. Chantepie, J. Villares, F. Lamari, E. Jospin, T. H. Van Kuppevelt, A. G. Mensah-Nyagan, R. Raisman-Vozari, N. Soussi-Yanicostas and D. Papy-Garcia, *Brain*, 2015, **138**, 1339–1354.
- 21 R. J. Holley, A. Deligny, W. Wei, H. A. Watson, M. R. Niñonuevo, A. Dagälv, J. A. Leary, B. W. Bigger, L. Kjellén and C. L. R. Merry, *J. Biol. Chem.*, 2011, **286**, 37515–37524.
- 22 S. Günal, R. Hardman, S. Kopriva and J. W. Mueller, *J. Biol. Chem.*, 2019, **294**, 12293–12312.
- 23 J. I. Armstrong, A. R. Portley, Y. T. Chang, D. M. Nierengarten, B. N. Cook, K. G. Bowman, A. Bishop, N. S. Gray, K. M. Shokat, P. G. Schultz and C. R. Bertozzi, *Angew. Chemie - Int. Ed.*, 2000, **39**, 1303–1306.
- 24 J. P. Bourdineaud, J. J. Bono, R. Ranjeva and J. V. Cullimore, *Biochem. J.*, 1995, **306**, 259–264.
- 25 D. E. Verdugo and C. R. Bertozzi, *Anal. Biochem.*, 2002, **307**, 330–336.
- 26 D. P. Byrne, Y. Li, K. Ramakrishnan, I. L. Barsukov, E. A. Yates, C. E. Eyers, D. Papy-Garcia, S. Chantepie, V. Pagadala, J. Liu, C. Wells, D. H. Drewry, W. J. Zuercher, N. G. Berry, D. G. Fernig and P. A. Eyers, *Biochem. J.*, 2018, **475**, 2417–2433.
- 27 N. M. Kershaw, D. P. Byrne, H. Parsons, N. G. Berry, D. G. Fernig, P. A. Eyers and R. Cosstick, *RSC Adv.*, 2019, **9**, 32165–32173.
- 28 S. E. Bodman, C. Breen, E. Robertson, S. Kirkland, S. Wheeler, F. Plasser and S. J. Butler, 2021, Manuscript submitted.
- 29 M. A. Beatty, J. Borges-González, N. J. Sinclair, A. T. Pye and F. Hof, *J. Am. Chem. Soc.*, 2018, **140**, 3500–3504.
- 30 A. Hennig, H. Bakirci and W. M. Nau, *Nat. Methods*, 2007, **4**, 629–632.
- 31 W. M. Nau, G. Ghale, A. Hennig, H. Bakirci and D. M. Bailey, *J. Am. Chem. Soc.*, 2009, **131**, 11558–11570.
- 32 Q. Chen, M. H. Zeng, Y. L. Zhou, H. H. Zou and M. Kurmoo, *Chem. Mater.*, 2010, **22**, 2114–2119.
- 33 Z. Kovacs and A. D. Sherry, *J. Chem. Soc. Chem. Commun.*, 1995, **1**, 185–186.
- 34 A. Beeby, I. M. Clarkson, R. S. Dickins, S. Faulkner, D. Parker, L. Royle, A. S. De Sousa, J. A. G. Williams and M. Woods, *J. Chem. Soc. Perkin Trans. 2*, 1999, 493–503.
- 35 T. R. Rudd and E. A. Yates, *Mol. Biosyst.*, 2012, **8**, 1499–1506.
- 36 L. Fu, K. Li, D. Mori, M. Hirakane, L. Lin, N. Grover, P. Datta, Y. Yu, J. Zhao, F. Zhang, M. Yalcin, S. A. Mousa, J. S. Dordick and R. J. Linhardt, *J. Med. Chem.*, 2017, **60**, 8673–8679.
- 37 K. Suzuki, A. Kobayashi, S. Kaneko, K. Takehira, T. Yoshihara, H. Ishida, Y. Shiina, S. Oishi and S. Tobita, *Phys. Chem. Chem. Phys.*, 2009, **11**, 9850–9860.
- 38 S. C. Edavettal, K. A. Lee, M. Negishi, R. J. Linhardt, J. Liu and L. C. Pedersen, *J. Biol. Chem.*, 2004, **279**, 25789–25797.

